

# SVPWM Technique for Cuk Converter

R. Lidha O R Maggie\* and E. Karpagavalli

Department of EEE, Dr. Sivanthi Aditanar College of Engineering, Thiruchendur - 628215,  
Tamil Nadu, India; iamlidha@gmail.com

## Abstract

The diode-assisted Cuk Voltage Source Inverter (VSI) enhances the voltage boost capability which is more suitable for wide range voltage regulation in dc/ac power conversion. This paper mainly describes Pulse-Width Modulation (PWM) strategy for diode-assisted cuk VSI. Compared with existing buck-boost converter, diode-assisted capacitor cuk VSI with SVPWM strategy demonstrates good performances like less switching device requirement and higher efficiency at high voltage gain. The proposed diode-assisted cuk VSI is more advantageous and competitive topology for wide range dc/ac power conversion in a renewable energy application. Simulation model of SVPWM is obtained using MATLAB/SIMULINK.

**Keywords:** DC-Link Voltage Utilization, Pulse-Width Modulation (PWM), Voltage Boost, Voltage Gain, Voltage Source Inverter (VSI), Voltage Stress

## 1. Introduction

For the sustainable development of economy and environment, solar cells and fuel cells as clean energy are promising in various power electronic applications in the future, such as battery back-up distributed power supply system, parallel connected photovoltaic generated power system, and fuel cells supplied motor drive system. The obvious characteristic in these applications is low dc source voltage supply with wide range voltage drop and high required output ac voltage<sup>1-3</sup>. Some applications raise new requirements for power electronic converters such as the capability of wide range voltage buck-boost, high efficiency. As for the traditional Voltage Source Inverter (VSI), the peak ac output voltage is lower than the available dc source voltage. Therefore, it can only perform the buck dc-ac power conversion and the maximum ac output phase voltage is limited to 1.15 times half of the dc source voltage using Sinusoidal Pulse-Width Modulation (SPWM) with third harmonic injection or Space Vector Modulation (SVM)<sup>5,6</sup>.

For applications requiring both buck and boost power conversion, conventional dc-dc buck-boost

VSI has been widely used for its simple structure and control technology. However, the switching devices in the front boost circuit bear large dc source current and high intermediate dc-link voltage under extreme larger voltage boost duty ratio<sup>1</sup>. In view of additional power conversion stage increasing system cost and reduced efficiency, the literature<sup>6</sup> proposed Z-source inverter. Z-source inverter introduces a unique impedance network between the source and the inverter to obtain both voltage buck and boost properties. It boosts the dc source voltage by adopting shoot-through operation mode, which provides a potential low-cost, reliable and single-stage approach for dc/ac power conversion when the voltage gain is low (1-2). Therefore, the switching devices in Z-source inverter bear large voltage stress and current stress than that in conventional dc-dc buck-boost VSI, especially under very high voltage gain applications. Although both of them can theoretically boost ac output voltage to any desired value without upper limitation, the degradation of efficiency and increasing requirement of semi conductor devices make them impractical under the conditions of very high voltage gain applications.

\*Author for correspondence

## 2. Existing Converter

The existing diode-assisted buck-boost VSI<sup>5</sup> shown in Figure 1 further extends the voltage transfer ratio and avoids the extreme duty ratio of switching device in the front boost circuit for wide range buck and boost power conversion. The new topology integrates an X-shaped diode-assisted capacitor network between the boost inductor and the inverter bridge. Since the diodes in the network are naturally conducting to perform parallel capacitive charging and are reverse-biased in the next interval to realize series capacitive discharging, the high voltage in the dc-link of the inverter bridge can be easily achieved with the same boost duty ratio and voltage rating of the capacitors.

Diode-assisted buck-boost VSI shown in Figure 1 has two operating modes according to the switching state of S1. For the convenience of analysis, the two capacitors C1 and C2 in the symmetrical X-shape network are assumed to have the same capacitance and terminal voltage.

Figure 2 shows the equivalent circuit of diode-assisted buck-boost VSI viewed from the dc link of the inverter bridge when S1 is turned ON. During this interval, the two diodes are reverse biased. Therefore, the inductor absorbs energy from the dc source by increasing the charging current and both of the capacitors are connected in series to supply the loads.

Figure 3 shows the equivalent circuits of diode-assisted buck-boost VSI viewed from the dc link of the inverter bridge when S1 is turned OFF. During this interval, the

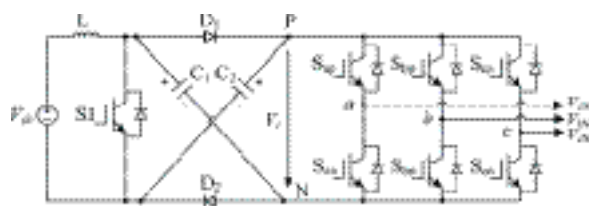


Figure 1. Diode-assisted buck-boost VSI.

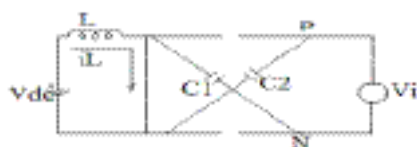


Figure 2. MODE 1 operation.



Figure 3. MODE-2 operation.

two diodes are forward biased. Therefore, the energy accumulated in the inductor is transferred to the capacitors and both the capacitors are connected in parallel to supply the loads.

## 3. Proposed Converter

Many years ago, Dr. Cuk invented the integrated magnetic concept called Dc-transformer, where the sum of Dc fluxes created by currents in the winding of the input inductor L1 and transformer T is equal to Dc flux created by the current in the output inductor L2 winding. Hence the Dc fluxes are opposing each other and thus result in a mutual cancellation of the Dc fluxes.

Cuk converter has several advantages over the buck converter. One of them Cuk converter provide capacitive isolation which protects against switch failure (unlike the buck topology). Other advantage is, the continuous input current of the Cuk converter, and the Cuk can draw a current free from ripple from a PV array that is an important one for efficient Maximum Power Point Tracking (MPPT).

As shown in Figure 4, in a Cuk converter, the main energy storage is the capacitor used. So, the input current is continuous. These circuits have high efficiency and low switching losses. Due to the inductor on the output stage, the Cuk converter can provide a better output current characteristic.

The circuit arrangement of the Cuk converter using MOSFET switch is shown in Figure 4 in case of Cuk converter the output voltage is opposite to input voltage.

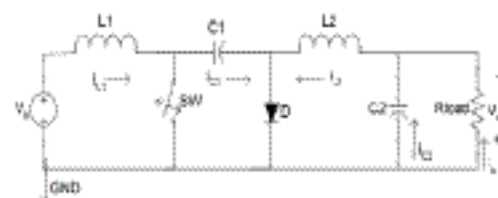


Figure 4. Circuit diagram of Cuk converter.

When the input voltage turned on and MOSFET (SW) is off, diode D is forward biased and capacitor C1 is charged through L1-D and here the operation of converter is divided into two modes.

### 3.1 Modes of Operation

As shown in Figure 5 When MOSFET switch is turned on at  $t = 0$ . The current through  $L_1$  rises. And at the same time the voltage of  $C_1$  reverse biases diode D and turn it off. The capacitor  $C_1$  discharges its energy to the circuit  $C_1$ - $C_2$ -load- $L_2$ .

As shown in Figure 6 when MOSFET switch is turned off at  $t = t_1$ . The capacitor will start to charge from input supply  $V_s$  and the energy stored in the inductor transferred to the load. The capacitor  $C_1$  is the medium for transferring energy from source to load.

## 4. SVPWM Technique

### 4.1 Three Phase Modelling Review

The power circuit topology of a three-phase VSI leg is composed of two back-to-back connected semiconductor devices. One of these two is a controllable device and other one is a diode for protection. Every inverter leg's state changes after an interval of  $60^\circ$  and their state remains constant for  $60^\circ$  interval. Thus it follows that the leg voltages will have six distinct and discrete values in one cycle ( $360^\circ$ ). Space vector representation of the three-

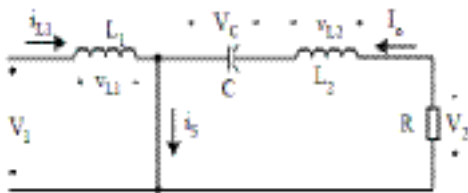


Figure 5. Mode 1 Operation.

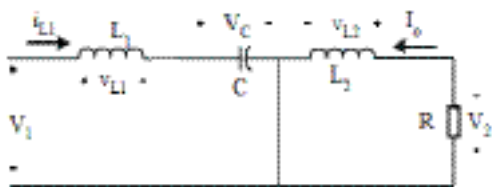


Figure 6. Mode 2 operation.

Table 1. Phase voltage values for switching states

State	Switch On	$v_A$	$v_B$	$v_C$
1	1,4,6	$(2/3)V_{dc}$	$-(1/3)V_{dc}$	$-(1/3)V_{dc}$
2	1,3,6	$(1/3)V_{dc}$	$(1/3)V_{dc}$	$-(2/3)V_{dc}$
3	2,3,6	$-(1/3)V_{dc}$	$(2/3)V_{dc}$	$-(1/3)V_{dc}$
4	2,3,5	$-(2/3)V_{dc}$	$(1/3)V_{dc}$	$(1/3)V_{dc}$
5	2,4,5	$-(1/3)V_{dc}$	$-(1/3)V_{dc}$	$(2/3)V_{dc}$
6	1,4,5	$(1/3)V_{dc}$	$-(2/3)V_{dc}$	$(1/3)V_{dc}$
7 & 8	1,3,5 2,4,6	0	0	0

phase inverter output voltages is introduced next. The space vector is a simultaneous representation of all the three-phase quantities. It is a complex variable and is a function of time in contrast to the phasors. Phase voltages are summarised in Table 1.

### 4.2 Space Vector PWM

Three-phase VSI generates eight switching states which include six active and two zero states. These vectors form a hexagon (Figure 7) which can be seen as consisting of six sectors spanning  $60^\circ$  each. The reference vector which represents three-phase sinusoidal voltage is generated using SVPWM by switching between two nearest active vectors and zero vectors. To calculate the time of application of different vectors, consider Figure 7, depicting the position of different available space vectors and the reference vector in the first sector.

In order to obtain fixed switching frequency and optimum harmonic performance from SVPWM, each leg should change its state only once in one switching period.

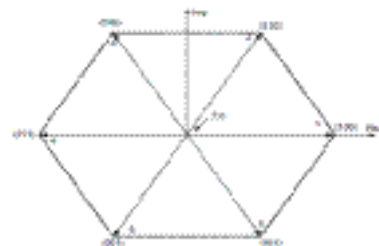


Figure 7. Phase voltage space vectors.

This is obtained by applying zero state vectors followed by two adjacent active state vectors in half switching period. The next half of the switching period is said to be the mirror image of first half. The total switching period is divided into 7 parts. The sinusoidal reference space vector forms a circular trajectory inside the hexagon. The magnitude of the output voltage can be increased by using SVPWM. The radius of the largest circle that can be inscribed within the hexagon is tangential to the mid points of the lines joining the ends of the active space vector.

## 5. Matlab/Simulink Model

Simulink model of the proposed converter is shown in Figure 8.

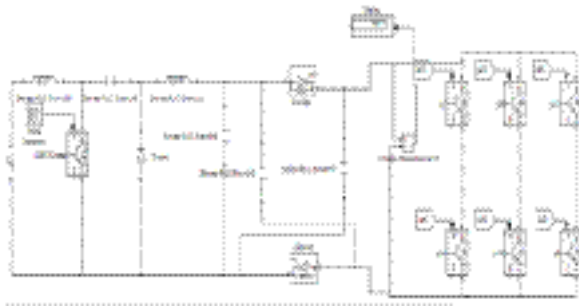


Figure 8. Simulation of proposed converter.

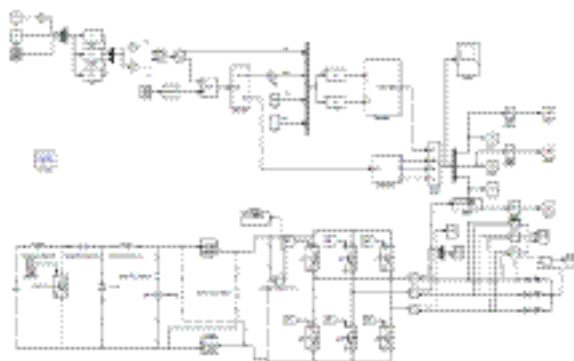


Figure 9. Entire simulation diagram.

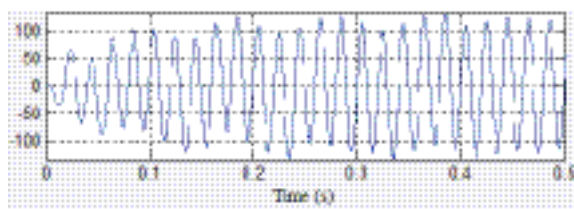


Figure 10. 3 Phase Line current.

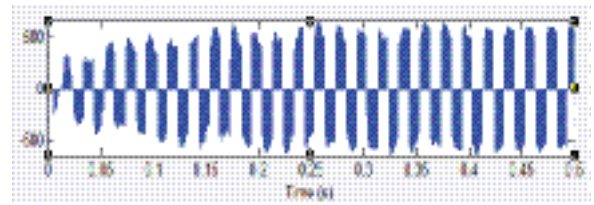


Figure 11. Phase voltage.

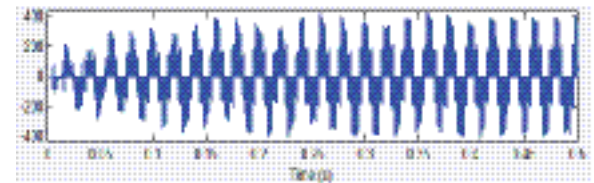


Figure 12. Line voltage.

## 6. Conclusion

This proposed diode-assisted Cuk inverters having a larger voltage gain, as compared to existing buck-boost inverters. The larger line voltage is exhibited by the proposed inverters is achieved by using a diode-capacitor network that can actively configure itself to perform parallel capacitive charging and series discharging is to give an immediate voltage multiplication factor of 2. For the input of 25V the output obtained is 517 V which is the twice of the dc-link voltage. THD is also reduced as 0.64% for line current, 6.72% for phase voltage and 6.77% for line voltage. Therefore, diode-assisted cuk VSI is a more promising and competitive topology for wide range power conversion in renewable energy applications.

## 7. References

1. Gao F, Loch PC, Teodorescu R, Blaabjerg F. Diode-assisted buck-boost voltage-source inverters. *IEEE Trans Power Electron.* 2009 Sep; 24(9):2057–64.
2. Peng FZ. Z-Source inverter. *IEEE Trans Ind Appl.* 2003 Mar; 39(2):504–10.
3. Nguyen M-K, Lim Y-C, Cho G-B. Switched-inductor quasi-Z source inverter. *IEEE Trans Power Electron.* 2011 Nov; 26(11):3183–91.
4. Hwu KI, Yau YT. Two types of KY buck-boost converters. *IEEE Trans Ind Electron.* 2009 Aug; 56(8):2970–80.
5. Gao F, Liang C, Loh PC. Buck-boost current-source inverters with diode-inductor network. *IEEE Trans Ind Appl.* 2009 Apr; 45(2):794–804.
6. Holmes DG, Lipo TA. *Pulse width modulation for power converters: principles and practice.* Hoboken, NJ: Wiley; 2003.

7. Blaabjerg F, Freysson S. A new optimized space-vector modulation strategy for a component minimized voltage source inverter. *IEEE Trans Power Electron.* 1997 Jul; 12(4):704–14.
8. Bazzi AM, Krein PT, Kimball JW. IGBT and diode loss estimation under hysteresis switching. *IEEE Trans Power Electron.* 2012 Mar; 27(3):1044–8.
9. Blaabjerg F, Pedersen J, Elkjaer A. An extended model of power losses in hard-switched IGBT inverters. *Proceedings 31st IAS Annual Meeting, Conference Record of IEEE Indian Applications Conference*; 1996. p. 3006–12.
10. Graovac D, Porsche M. IGBT power losses calculation using the data-sheet parameters. *Technical Report, Applications Notes.* Germany: Infineon Neubiberg; 2006 Jul. p. 3–6.